NASA TN D-1146

TECHNICAL NOTE

D-1146

EFFECTS OF SURFACE RECOMBINATION ON HEAT TRANSFER TO BODIES IN A HIGH ENTHALPY STREAM OF PARTIALLY DISSOCIATED NITROGEN

By Ernest L. Winkler and Roy N. Griffin, Jr.

Ames Research Center
Moffett Field, Calif.

NATIONAL AERONAUTICS AND SPACE ADMINISTRATION
WASHINGTON
December 1961

NATIONAL AERONAUTICS AND SPACE ADMINISTRATION

TECHNICAL NOTE D-1146

EFFECTS OF SURFACE RECOMBINATION ON HEAT TRANSFER TO BODIES IN A HIGH ENTHALPY STREAM OF PARTIALLY DISSOCIATED NITROGEN

By Ernest L. Winkler and Roy N. Griffin, Jr.

SUMMARY

Heat-transfer rates to two surfaces having widely different catalytic effectiveness are compared at a Mach number of 6 in a low-density stream of partially dissociated nitrogen. The heat-transfer rate to a polished copper cylinder is twice as great as the heat-transfer rate to a silicon-monoxide-coated cylinder when the stream total energy content is 9000 Btu/lb. Various methods for determining the stream energy content, the stream velocity, and the stream Mach number have been developed and compared. It is shown that methods for estimating the stream energy content by means of purely aerodynamic concepts may neglect the sizable fraction of the stream energy contained in molecular dissociation.

INTRODUCTION

In certain regimes of high-speed flight, the gas behind the bow wave of a vehicle is frozen in a dissociated state, and the surface heat-transfer rate can then be strongly influenced by recombination of the dissociated atoms at the surface. This surface recombination with its attendant energy release raises the heat-transfer rate to a higher value than that which would occur if no recombination were to take place. As has been shown in reference 1, the catalytic activity of the surface, in many situations of interest, will determine the recombination rate. Although ground-based equipment can simulate these hypersonic flight conditions only in an imperfect manner, it is possible to operate certain arc-heated wind tunnels so that at least some of the effects of surface catalysis on heat transfer can be observed. For such observations to be meaningful, however, it is a necessary prerequisite that the state properties of the total stream be well defined.

Of the many papers on the subject of heat transfer in a dissociated gas stream, those that typically represent the present status of knowledge are the theoretical analyses of references 2, 3, and 4 and the experimental results of reference 5. References 6, 7, and 8 are typical of the many papers that discuss the methods and techniques of measuring the state properties of a high-enthalpy gas stream. Measurements reported in these papers have included heat transfer to a stagnation point, total pressure in the nozzle plenum chamber, static pressure, and impact pressure. From

these measurements, attempts have been made to calculate various stream parameters, such as enthalpy level, Mach number, and temperature. Unfortunately, none of the results of these investigations, taken separately or together, afford a means for a definitive evaluation of the effects of surface recombination on heat transfer.

The purposes of the present investigation are to study the effects of surface catalysis on heat transfer in a low density, high enthalpy stream of partially dissociated diatomic gas and concurrently to determine the relevant gas properties by various independent methods of measurement. These purposes will be accomplished by presentation of results from experiments performed in an electric-arc-heated, supersonic stream of dry nitrogen, so operated as to be out of thermodynamic equilibrium with respect to homogeneous reactions. Because of the small model size, the results obtained are of limited interest with regard to actual flight situations of interest. The methods and techniques herein presented should prove to be of utility in future investigations of this nature.

SYMBOLS

a	speed of sound
B	magnetic field strength
c	atom mass fraction
c_v	specific heat at constant volume
c_p	specific heat at constant pressure
d	distance separating electrode tips
E	voltage
f_j	degrees of freedom of the jth species of gas particle
g	gravitational constant
h	enthalpy
h_R	heat of atomic recombination
J	mechanical equivalent of heat
k_w	catalytic reaction rate constant
K.E.	kinetic energy
Le	Lewis number

m_j mol fraction of the jth species

M Mach number

M_j mol weight of the jth species

$\bar{M}$ average mol weight

M_o initial mol weight of the unheated gas

N total number of data points

A 4 7 0 N_u number of data points showing a velocity less than a given velocity u

p pressure

q_{k_w} heat-transfer rate to a wall having a catalytic reaction rate constant of k

$\bar{q}$ ratio of heat-transfer rates, $\frac{q_{k_w}}{q_{k_w=\infty}}$

R gas constant

R universal gas constant

T temperature

u gas velocity

$\dot{w}$ weight rate of gas flow

z compressibility, $\frac{M_o}{\bar{M}}$ or $\frac{pM_o}{\rho RT}$

Γ effective expansion coefficient defined by $p\rho^{-\Gamma} = \text{constant}$

φ correction factor for catalytic effects

ρ gas density

Subscripts

e conditions at the edge of the boundary layer

j general jth species of gas component

t total conditions

SiO	silicon-monoxide surface
se	stagnation conditions at the outer edge of the boundary layer
Cu	copper surface
1	free-stream conditions
2	conditions behind a shock wave
∞	infinity

APPARATUS AND PROCEDURE

The Wind Tunnel

The tests were carried out in a high-enthalpy, low-density, supersonic wind tunnel. Dry nitrogen was heated by passage through a direct-current electric arc produced by a commercially available arc heater. From the arc heater, the gas discharged at essentially constant pressure into a water-cooled plenum chamber and then expanded through a water-cooled, axially symmetric nozzle. The nozzle contour was designed for a nominal Mach number of 6 under cold flow conditions. From the nozzle, the gas stream discharged as a 4-inch-diameter open jet into a test chamber which was evacuated by a five-stage, stream-driven ejector system. The test section pressure was matched to the stream static pressure by throttling at the entrance to the steam ejectors. Figure 1 is a diagrammatic sketch of the arc heater, plenum chamber, nozzle, and test chamber.

In all the tests, the gas used was dry, oil free, nitrogen. The nitrogen flow rate through the arc heater and nozzle was always 0.0054 pound per second as measured by a rotameter. A choked orifice in the gas line, downstream of the throttle valve, prevented variations in arc-chamber pressure from affecting the flow rate.

INSTRUMENTATION

Pressure Measurements

Pressures were measured with strain-gage-type pressure cells, with signal read-out on either a strain-gage amplifier-recorder unit or an automatic plotting system. The strain-gage amplifier-recorder system was used to record the total pressure in the plenum chamber and the stream static pressure. Impact pressure surveys of the stream were made with a 1/2-inch-O.D., water-cooled impact pressure tube using the automatic plotting system to measure the variation of the impact pressure with position across the stream. These surveys were made at a position

1 inch downstream of the nozzle. The plenum chamber stagnation pressure was measured at a tap in the side wall, and the assumption is made that the pressure so measured does not depart significantly from the total pressure. Calibrations at static conditions just prior to each set of measurements allowed the absolute magnitude of the various pressures to be determined by the use of suitable scale factors.

POWER AND ENERGY REQUIREMENTS

Input power to the arc heater was determined from the product of arc current and arc-voltage drop as measured on moving coil, direct-current meters of the D'Arsonval type.

Energy losses were evaluated by measuring the flow rate and temperature rise of the cooling water to the arc heater, plenum chamber, and nozzle. The water flow rates were measured with rotameters and the temperature rise was measured by differential thermopiles and recorded on an oscillograph.

VELOCITY MEASUREMENTS

By virtue of the partial ionization of the stream, direct measures of the stream velocity were possible by three methods. The first method consisted of an application of Faraday's generator rule wherein the potential developed by a conductor (in this case the partially ionized gas stream) moving through a magnetic field of known strength provided a measure of the velocity. The 4-inch-diameter ionized stream was passed through the uniform field developed between the poles of an electromagnet at right angles to the lines of flux. The electromotive force generated by virtue of the stream velocity was detected by means of two 1/8-inch-diameter cylindrical electrodes inserted coaxially into opposite edges of the stream at right angles to both the magnetic-flux vector and the stream-velocity vector. From the measured field strength B (gauss), the measured distance separating the electrodes d (cm), and the measured voltage E, the stream velocity could be calculated from Faraday's law, namely, $u = E \times 10^8 / B \times d$, cm/sec.

The two other methods depended on measuring the time for random pulsations of the stream caused by inherent arc power fluctuations to travel a measured distance in the flow direction. In the first of these, two Langmuir probes detected the stream potential pulsations caused by nonuniform stream ionizations; in the second, two photomultiplier tubes detected variations in stream luminosity. In both cases, the signals were displayed on a dual beam oscilloscope. The sweep of the oscilloscope was triggered by the 35-mm movie camera used to photograph the traces.

From the sweep speed, the phase relationship of the traces, and the distance separating the detectors, the stream velocity could be calculated. A complete explanation of the method is given in appendix A.

STAGNATION-POINT HEAT-TRANSFER MEASUREMENTS

Stagnation-point heat-transfer rates were measured with 1/2-inch-diameter heat-transfer probes. An 0.898-gm slug of copper with a 0.3-inch-diameter face was placed at the axisymmetric stagnation region and was thermally insulated from the body of the probe. (See fig. 2(a).) The variation of the temperature of this slug with time was recorded on an oscillograph. The stagnation point of the test probe was placed on the stream axis at a position 1 inch downstream of the nozzle exit plane. The heat transfer was calculated from the known mass, the frontal area, and the time-temperature history of the slug.

STREAM CALIBRATION

Calibrations of the test stream were made over a 2-to-1 range of input power levels to the arc heater. The total pressure and static pressure were measured and, in addition, impact pressure surveys were made at three power levels which bracketed the usable range of the nozzle and arc heater. Determinations of the energy content of the gas were made from

(1) an energy balance,
(2) calculations based on critical sonic flow relationships,
(3) an effective-expansion-exponent method which is described in detail in appendix B,
(4) heat-transfer measurements and the theories of references 1 and 4, and
(5) velocity measurements.

Methods (1) and (2) provide bulk or average measures of energy content, method (3) provides an average energy content for that portion of the stream that is unaffected by the nozzle boundary layer, whereas methods (4) and (5) provide essentially local values on the stream center line.

The energy balance was made by subtracting the losses to the cooling water from the total energy input. To include the heat stored in the masses of the arc heater, plenum chamber, and nozzle, the time-integrated product of the cooling water flow rate and its temperature rise was evaluated. The integration was made from the time the arc heater was started until after the power was off when no difference between inlet and outlet

cooling water temperatures could be detected. The difference between the total energy input and the losses divided by the total mass flow of the gas during the test gave the average total energy content of the gas stream.

Two sonic flow methods were used to calculate the enthalpy of the gas. Both methods can be derived from solutions of the one-dimensional continuity, momentum, and energy equations for compressible inviscid flow. These solutions give relationships between stagnation pressure and stream enthalpy for a given gas flow rate and nozzle throat area. The equilibrium sonic flow method is based on the real gas properties of nitrogen and assumes that the gas expands isentropically in complete chemical and thermodynamic equilibrium from the plenum chamber to the sonic point which is assumed to be at the minimum area of the nozzle. The second method, the frozen sonic flow method, is based on an assumed calorically perfect gas having the same properties as the hot gas in the plenum chamber. In this method, the composition and vibrational energy of the gas were assumed to be unchanged from the plenum chamber to the sonic point. Thus, a constant effective expansion exponent can be used in the polytropic gas law.

The heat-transfer rate measured with the heat-transfer probe described earlier was also used to provide a measure of the stream enthalpy. This method is based on the laminar boundary-layer heat-transfer solution of reference 3. It was initially assumed that the atom recombination rate at the calorimeter surface was infinite. A correction of about 15 percent for a finite recombination rate based on the catalytic wall recombination rate given in reference 1 was later applied. An iterative procedure was required to make this correction since the recombination rate is a function of the stream enthalpy.

The method for the determination of the effective expansion exponent for frozen flow was also used to calculate the stream enthalpy. This method is based on the assumptions that the local Mach number is unique and that the effective expansion exponent, Γ, is invariant from the point at which the flow freezes to the mouth of the impact pressure probe. A complete description of the method is given in appendix B.

The translational kinetic energy per pound of gas of the stream can be calculated using the measured values of the stream velocity

$$\frac{\text{K.E.}}{\dot{w}} = \frac{u^2}{2gJ} \tag{1}$$

This fraction of the total energy neglects all of the intrinsic energy contained in molecular translation, vibration, and rotation, molecular dissociation, and ionization.

Heat-Transfer Apparatus

The heat-transfer tests were made by comparing the heat-transfer rate to 1/4-inch-diameter, water-cooled, cylindrical, copper tubes having surfaces of different catalytic effectiveness. The tubes were placed, a pair at a time, transversely to the stream in symmetrical positions with respect to the stream axis. The polished exterior of the basic copper tubes served as the most active surface, whereas those with the lowest activities were surfaced with vacuum-deposited layers of silicon monoxide approximately 5000 Å thick. These materials were chosen because of their ready availability and their widely different catalytic activity (ref. 1). Figure 2(b) is a sketch of this apparatus and its location with respect to the test stream.

The heat-transfer rate to each tube was calculated from the cooling water flow rate and its temperature rise at steady-state condition. Cooling water flow rates were measured by two identical rotameters, and an oscillograph was used to record the signal from differential thermocouples to give a measure of the cooling water temperature rise.

To preclude the possibility that systematic asymmetries in the test stream might influence the results, check runs were carried out with two uncoated tubes at the start of the test series and at a point approximately at the midpoint of the series. In addition, thermocouple sets were switched from one tube to the other in similar check runs with uncoated tubes. The test specimens extended completely across the stream, so that necessarily a portion of each tube was in the nozzle boundary layer where conditions differed considerably from those of the stream core.

RESULTS AND DISCUSSION

Stream Properties

A plot of impact pressure ratio variation with distance from the nozzle axis for test conditions at three levels of arc energy input is shown in figure 3. The impact pressure surveys were made at a position 1 inch downstream of the nozzle exit plane. The parameter used in this plot is the arc energy input in Btu per pound of gas which is defined as 0.948 kilowatt/$\dot{w}$. A comparison of these stream impact pressure profiles shows that as the arc energy input per pound of gas increases, the region of uniform impact pressure decreases in diameter until it is practically nonexistent at the arc energy input level of 11,870 Btu/lb. This may be attributed to growth of the boundary layer in the nozzle. A similar effect in an undissociated gas stream arises from the failure of the nozzle to maintain an isentropic core. Figure 4 is a plot of the Mach number distribution in the nozzle. This Mach number is calculated

from the Rayleigh pitot equation using the data from the previously mentioned pressure surveys combined with the expansion exponent calculated by means of the method described in appendix B.

Energy Content

The results of measurements of the stream energy content by the energy balance, effective-expansion-exponent, and stagnation-point heat-transfer methods at various arc energy input levels are shown in figure 5.

A
4
7
0

The energy balance method provides a measure of the average total energy of the gas stream. Since no assumptions are made in determining the stream energy by this method, it is considered to represent the average total energy in the gas in all forms.

The effective-expansion-exponent method (appendix B) provides a measure of the enthalpy of the stream core. Because of energy losses from the boundary layer (which are measured in the energy balance method), the enthalpy as deduced by this method should be higher than the average total stream energy content. It can be seen in figure 5 that this is the case except for the test point at the highest energy input level. At this energy input level it can be seen on figure 3 that the flow is approaching pipe flow, thus violating the assumptions of appendix B.

The enthalpy deduced from stagnation-point heat-transfer methods is also shown on figure 5. Calculations of the stream enthalpy were made on the basis of infinite and finite calorimeter surface activity. The enthalpy calculated on the basis of the finite surface activity of copper indicates that the enthalpy along the stream axis is somewhat higher than the average stream energy content. This is in agreement with the previous discussion. The enthalpy computed on the assumption of infinite surface activity approximates the energy content as measured by means of the energy balance.

Figure 6 is a plot of the stream velocity variation with arc energy input per pound of gas. In this figure are shown the results of three methods of measuring the stream velocity, namely, the application of the generator effect, and the electrical pulse-speed and the luminosity pulse-speed methods. Compared with these measured values of stream velocity are the results of calculations based on the speed of sound and the Mach number derived from the method of appendix B. Also shown in figure 6 are the theoretical velocities which would be attained by gases accelerating through a nozzle to a Mach number of 5.65 from conditions in a plenum chamber corresponding to a total energy based on the best fit curve of figure 5. The curve marked equilibrium flow is calculated on the assumption that the gas is in complete thermodynamic equilibrium whereas that marked frozen flow assumes that the gas is

thermally and calorically perfect with an invariant composition. Since the calculated velocity based on a gas in equilibrium is considerably higher than the measured value, this is additional evidence that the gas is not in equilibrium.

Although the approximate magnitude of the stream velocity is indicated by the various methods of measurement, more work remains to be done with the instrumentation before accurate velocity measurements can be obtained.

The data from both the electrical and luminosity pulse-speed methods of velocity measurement required analysis by statistical means as discussed in appendix A. Consequently, these methods appear to be less useful research tools for stream velocity measurements than the generator effect. The generator effect instrumentation is also better adapted to local stream velocity measurements than either of the other methods.

A 4 7 0

The variation of the kinetic energy of the stream with arc input energy per pound of gas is shown in figure 7. This kinetic energy is calculated from the velocity data presented in figure 6. It should be noted that the most probable velocity as calculated by the method of appendix A was used. Compared with this is the stream enthalpy calculated from critical sonic-throat concepts. The agreement between the values of the kinetic energy and the calculated critical sonic throat enthalpies shows that any determination of energy content that disregards internal and chemical forms of energy is likely to neglect a sizable portion of the total energy of the gas. This is emphasized by comparing the kinetic energy and the enthalpy calculated from critical sonic-throat concepts with the best fit curve of the total energy content from figure 5. In addition, it can be seen that the sonic-throat methods can be used to provide a measure of the energy available for conversion to kinetic form by expansion through a nozzle.

The kinetic energy of the gas calculated from results obtained by the method of appendix B is also shown in figure 7. It can be seen that this method can be used to indicate the relative proportions of the kinetic and intrinsic fractions of the total energy content of the gas.

Heating Rate to Catalytic and Noncatalytic Cylinders

Figure 8 shows the effects of a difference in surface catalytic effectiveness on the heating rate to cylinders in a frozen, partially dissociated, nonequilibrium nitrogen stream. As can be seen from this figure, the heat-transfer rate to the silicon-monoxide-coated cylinder is considerably lower than the rate to the copper cylinder.

Reference 1 gives the ratio for the heat-transfer rate to a surface of finite catalytic activity and the rate to a surface of infinite activity as

$$\bar{q} = \frac{q_{k_w}}{q_{k_w = \infty}} = 1 - \left[\frac{Le^{2/3}(h_R c_e/h_{se})}{1 + (Le^{2/3} - 1)(h_R c_e/h_{se})}\right](1 - \varphi) \qquad (2)$$

Assuming the value of k_w for silicon monoxide to be the same as that of Pyrex which was available in the literature, and having the value of k_w for copper, it is possible to calculate

$$\frac{\bar{q}_{SiO}}{\bar{q}_{Cu}} = \frac{1 + (h_R c_e/h_{se})(Le^{2/3}\varphi_{SiO} - 1)}{1 + (h_R c_e/h_{se})(Le^{2/3}\varphi_{Cu} - 1)} \qquad (3)$$

A 4 7 0

for the range of stream conditions covered in the tests. In addition to the previously noted assumptions, the following assumptions were made:

1. The copper surface was not oxidized.

2. The chemical and physical properties of the nozzle boundary layer were the same as those at the stream core.

A comparison of the experimental values of this ratio and the theoretical ratio is shown in figure 9. As the stream enthalpy increases, it can be seen from figure 9 that the effects of surface catalysis increase. At an energy content of 9000 Btu/lb, it is seen that the heat-transfer rate to a Pyrex surface should be approximately 40 percent of the heat-transfer rate to a polished copper surface. This effect was not quite realized in the experiments which show the decrease in heat-transfer rates to a silicon-monoxide-coated surface to be 50 percent of that to a copper surface. The agreement between theory and experiment indicates that large reductions in heat-transfer rate may be realized from the choice of a suitable noncatalytic surface for a re-entry vehicle.

CONCLUSIONS

Measurements have been carried out to compare various methods of determining the state properties of an electric-arc-heated stream of dissociated nitrogen, and to assess the effects of surface recombination on heat transfer to cylinders that differ widely in catalytic effectiveness. From an analysis of these measurements the following conclusions can be drawn:

1. Approximately half of the energy delivered to the nitrogen in the plenum chamber at a pressure of 1/3 atmosphere is unavailable for conversion to kinetic energy of mass motion when expanded through the nozzle at a total energy content of 9000 Btu/lb.

2. Sonic-throat methods of evaluating the energy content of an electric-arc-heated, supersonic gas stream may neglect large fractions of the total energy content of the gas.

3. Various fractions of the frozen energy may reappear at stagnation points in the supersonic stream, depending upon the catalytic effectiveness of the surfaces.

4. The heat-transfer rate to a surface of silicon monoxide can be 50 percent lower than the rate to a surface of polished copper when the stream energy content is about 9000 Btu/lb where approximately 19 percent of the mass of the nitrogen is dissociated.

Ames Research Center
National Aeronautics and Space Administration
Moffett Field, Calif., Sept. 15, 1961

APPENDIX A

TECHNIQUES FOR MEASURING THE VELOCITY OF AN ARC-HEATED, HIGH-ENTHALPY GAS STREAM

Because of inherent random fluctuations in the arc voltage causing variations in the energy input to an arc-heated gas stream, some disturbances may appear in the stream. Methods of measuring the speed of these disturbances may be used to determine the stream speed if the following conditions are approximated:

1. The disturbances travel downstream at the speed of the gas.

2. The measuring devices do not interfere with the stream.

The disturbances used in the speed measurements presented in this report are variations in the ionization level and the stream luminosity.

The variation of ionization level is detected by stagnation-point Langmuir probes inserted into the stream. These probes were copper wires insulated everywhere but at the ends. They were separated by approximately 1 inch in the flow direction and just far enough apart in the transverse direction to insure no mutual shock-wave interference at the electrically conducting tips.

Variations in stream luminosity were detected by two photomultipliers sighted across the stream through collimator tubes. The separation distance of these tubes in the flow direction was accurately measured. This spacing was approximately 2 inches.

Tests were made using each technique separately since the recording equipment was the same. In both cases the signals from the pair of detectors were displayed on a dual-beam oscilloscope. This display was recorded by a 35-mm movie camera which triggered the horizontal sweep of the beams. Each frame of the exposed film was examined to find those pairs of traces that had identical shapes. The remaining frames were discarded. The velocity of the disturbances could be calculated from the oscillograph sweep speed, the spacing of the detectors, and the phase relationship of the traces.

Both methods indicated stream velocities varying from 5,000 to over 30,000 feet per second, so a statistical method was used to analyze the results. A plot was made of the ratio of the number of data points showing a velocity below a given value to the total number of data points

as a function of the velocity. An example of this curve is shown in sketch (a). Here the line is a curve faired through the data points.

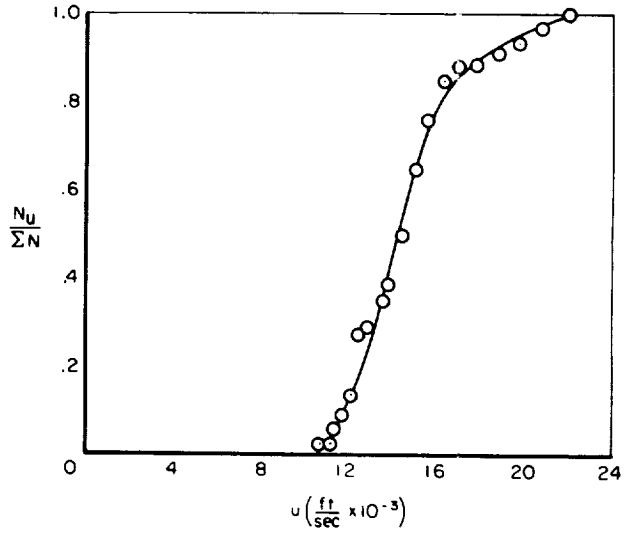

Sketch (a).- Fraction of data points showing a velocity less than u as a function of u; power input 12,100 Btu/lb.

The derivative of the curve was taken with respect to u and plotted as $\frac{d}{du}\left(\frac{N_u}{\Sigma N}\right)$ vs. u as shown in sketch (b). The most probable stream velocity was then taken at the maximum point of this curve.

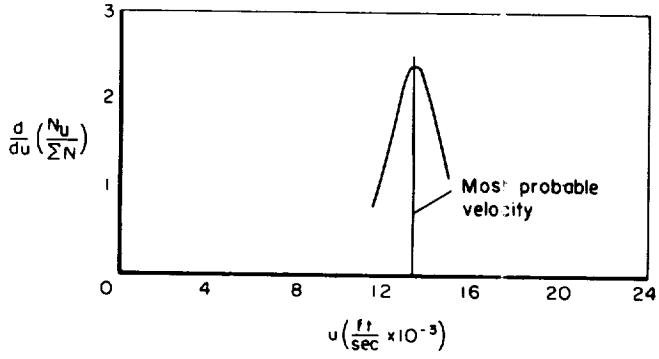

Sketch (b).- Derivative with respect to u of the curve shown in sketch (a); power input 12,100 Btu/lb.

APPENDIX B

A METHOD OF ESTIMATING THE ENTHALPY OF A FROZEN, PARTIALLY DISSOCIATED, ARC-HEATED GAS STREAM BY MEANS OF AN EFFECTIVE EXPANSION EXPONENT

This method is based on the validity of the following assumptions:

A 4 7 0

1. The stream core is quasi-isentropic; that is, the frozen, dissociated stream acts as if it were composed of an invariant mixture of perfect gases in isentropic flow.

2. The gas enthalpy is such that the gas is partially dissociated with the mass fraction dissociated between 0 and 1.

3. The effective expansion exponent, Γ, from the polytropic expansion equation $p\rho^{-\Gamma} = \text{const.}$ is unchanged from the point where the gas composition freezes, through the shock wave to the stagnation point of the impact probe.

The first of these assumptions is required when the isentropic expansion equations are used; the second is required because of the indeterminacy of the solution where $(d\Gamma/dT) = 0$. The third assumption is implied in the statement that the stream is frozen. In most cases of frozen flow, the stream will freeze in the region of the nozzle throat, but because of the weakness of the effects of pressure on recombination, it can usually be assumed that freezing takes place at the total stagnation pressure.

The following measurements must be made:

1. Free-stream static pressure, p_1
2. Total stagnation pressure, p_{t_1}
3. Stagnation pressure behind a normal shock wave, p_{t_2}

Two equations involving these pressures are available to solve for the two unknowns M and Γ:

$$\frac{p_{t_2}}{p_{t_1}} = \left[\frac{(\Gamma + 1)M_1^2}{(\Gamma - 1)M_1^2 + 2}\right]^{\frac{\Gamma}{\Gamma-1}} \left[\frac{\Gamma + 1}{2\Gamma M_1^2 - (\Gamma - 1)}\right]^{\frac{1}{\Gamma-1}} \tag{B1}$$

$$\frac{p_{t_2}}{p_1} = \left[\frac{(\Gamma + 1)M_1^2}{2}\right]^{\frac{\Gamma}{\Gamma-1}} \left[\frac{\Gamma + 1}{2\Gamma M_1^2 - (\Gamma - 1)}\right]^{\frac{1}{\Gamma-1}} \tag{B2}$$

These are equations (99) and (100) from reference 9 with the polytropic exponent Γ substituted for the isentropic γ.

Since the Mach number and the expansion exponent, Γ, are unique under the assumptions expressed previously, the simultaneous solution to these equations provides an expansion exponent which will be a function of the temperature at which the gas composition freezes. The equations given in reference 10

$$\Gamma = 1 + \frac{zR}{c_v} \quad \text{and} \quad c_v = \frac{R}{2} \Sigma_j \frac{\pi_j f_j}{M_j}$$

A
4
7
0

and equilibrium gas properties from tables and charts similar to those of reference 11 can be used to prepare a curve of Γ as a function of temperature at the stagnation pressure. The temperature at which the gas freezes in composition is then determined through Γ; hence, all the gas properties can be found through the use of tables and charts similar to those of reference 11. It must be noted that these are equilibrium charts and are correct only to the point where the gas departs from equilibrium.

By using the frozen flow equations $\alpha^2 = \Gamma zRT$ and $c_p = c_v + zR$ from reference 10, the stream velocity and intrinsic energy aside from the energy of dissociation can be calculated by means of the standard, one-dimensional isentropic equations.

Stream properties calculated by means of this method are presented in table I.

REFERENCES

1. Goulard, Robert J.: On Catalytic Recombination Rates in Hypersonic Heat Transfer. Jet Propulsion, vol. 28, no. 11, Nov. 1958, pp. 737-745.

2. Chambre, Paul L., and Acrivos, Andreas: On Chemical Surface Reactions in Laminar Boundary Layer Flows. Journal of Applied Physics, vol. 27 no. 11, March 1956, pp. 1322-1328.

3. Fay, James A., and Riddell, F. R.: Theory of Stagnation Point Heat Transfer in Dissociated Air. Jour. Aero. Sci., vol. 25, no. 2, Feb. 1958, pp. 73-85.

4. Chung, Paul M., and Anderson, Aemer D.: Heat Transfer to Surfaces of Finite Catalytic Activity in Frozen, Dissociated, Hypersonic Flow. NASA TN D-350, 1961.

5. Cutting, John C., Fay, James A., Hogan, William T., and Moffatt, W. Craig.: Heat Transfer in Dissociated Combustion Gases. AFOSR-TR-59-78, July 1959.

6. Brogan, Thomas R.: The Electric Arc Wind Tunnel. A Tool for Atmospheric Re-entry Research. A.R.S. Journal, Sept. 1959, pp. 648-652.

7. Nagamatsu, Henry J., Geiger, Ronald R., and Sheer, R. E., Jr.: Hypersonic Shock Tunnel. General Electric Rep. 59-RL-2164.

8. Buhler, Rolf D.: Hyperthermal Research Tunnel Development and Transport Property Measurements. Plasmadyne Corporation Rep. A-1 FR 119-1313, 4 Nov. 1959.

9. Ames Research Staff: Equations, Tables, and Charts for Compressible Flow. NACA Rep. 1135, 1954.

10. Geiger, R. E.: On the Frozen Flow of a Dissociated Gas. Jour. Aero-Space Sci., vol. 26, no. 12, Dec. 1959.

11. Hansen, C. Frederick: Approximations for the Thermodynamic and Transport Properties of High Temperature Air. NACA TN 4150, 1958.

TABLE I.- THERMODYNAMIC AND TRANSPORT PROPERTIES OF THE GAS STREAM CALCULATED FROM RESULTS OF THE EFFECTIVE-EXPANSION-EXPONENT METHOD

Arc power (Btu/lb of gas) . . .	6,920	9,120
p_{t_1}, psia	+.97	5.455
p_{t_2}, psia	0.220	0.256
p_1, psia	0.00526	0.00592
M	5.63	5.69
Γ	1.44	1.45
T_t, $^{\circ}R$	10,350	10,750
z, $(M_o/\bar{M})$	..15	1.19
T_1, $^{\circ}R$	1,340	1,300
c_v, Btu/lb $^{\circ}F$	0.194	0.196
c_p, Btu/lb $^{\circ}F$	0.279	0.285
c_pT_1, Btu/lb	374	371
u_1, ft/sec	11,100	11,350
Total enthalpy, Btu/lb.	5,470	6,610
$u_1^2/2gJ$, Btu/lb	2,450	2,670

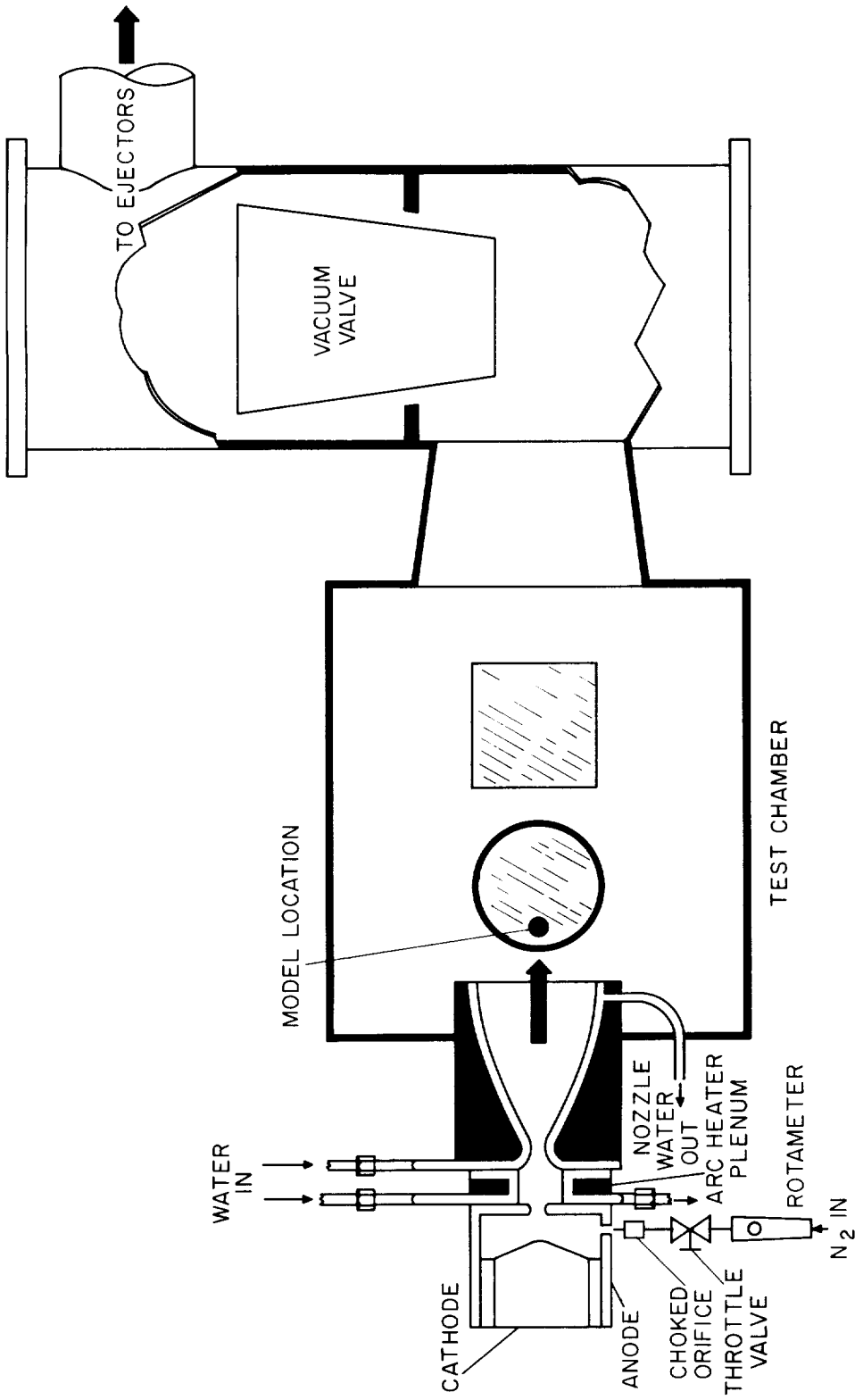

Figure 1.- Schematic diagram of the arc-heated wind tunnel.

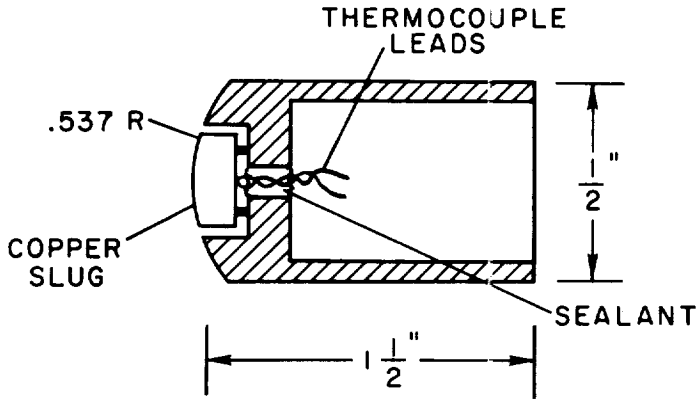

(a) Stagnation-point heat-transfer probe.

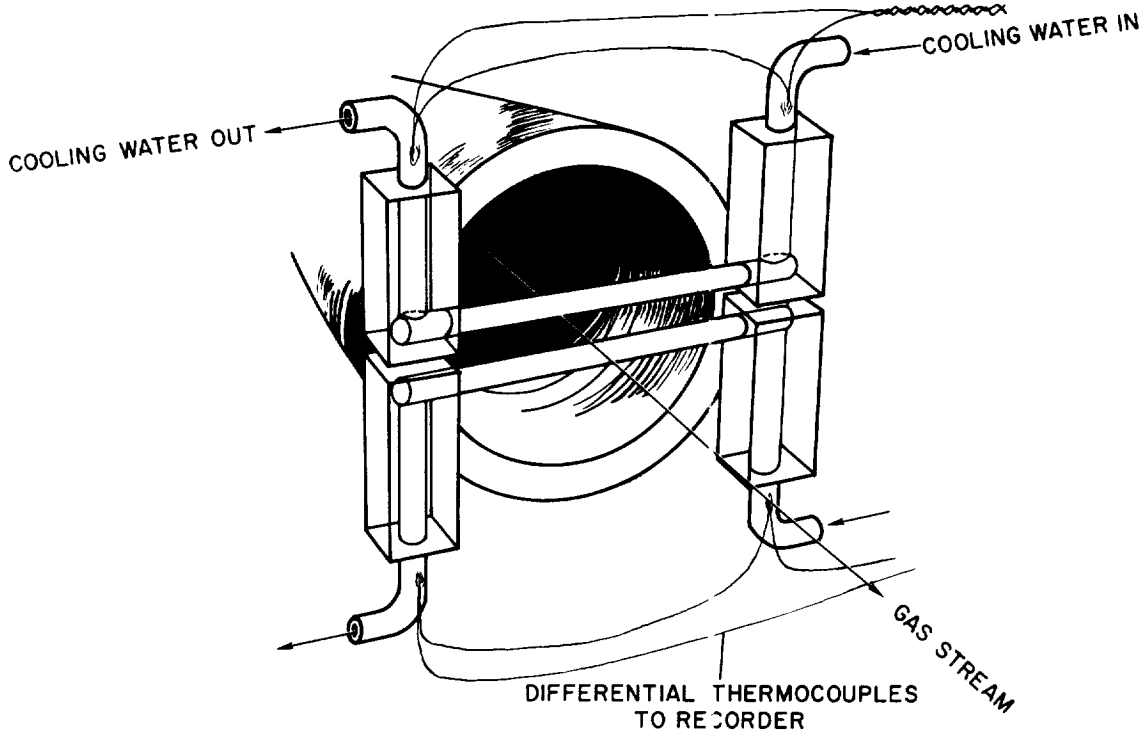

(b) Diagramatic sketch of catalytic effect heat-transfer apparatus.

Figure 2.- Heat-transfer measuring equipment.

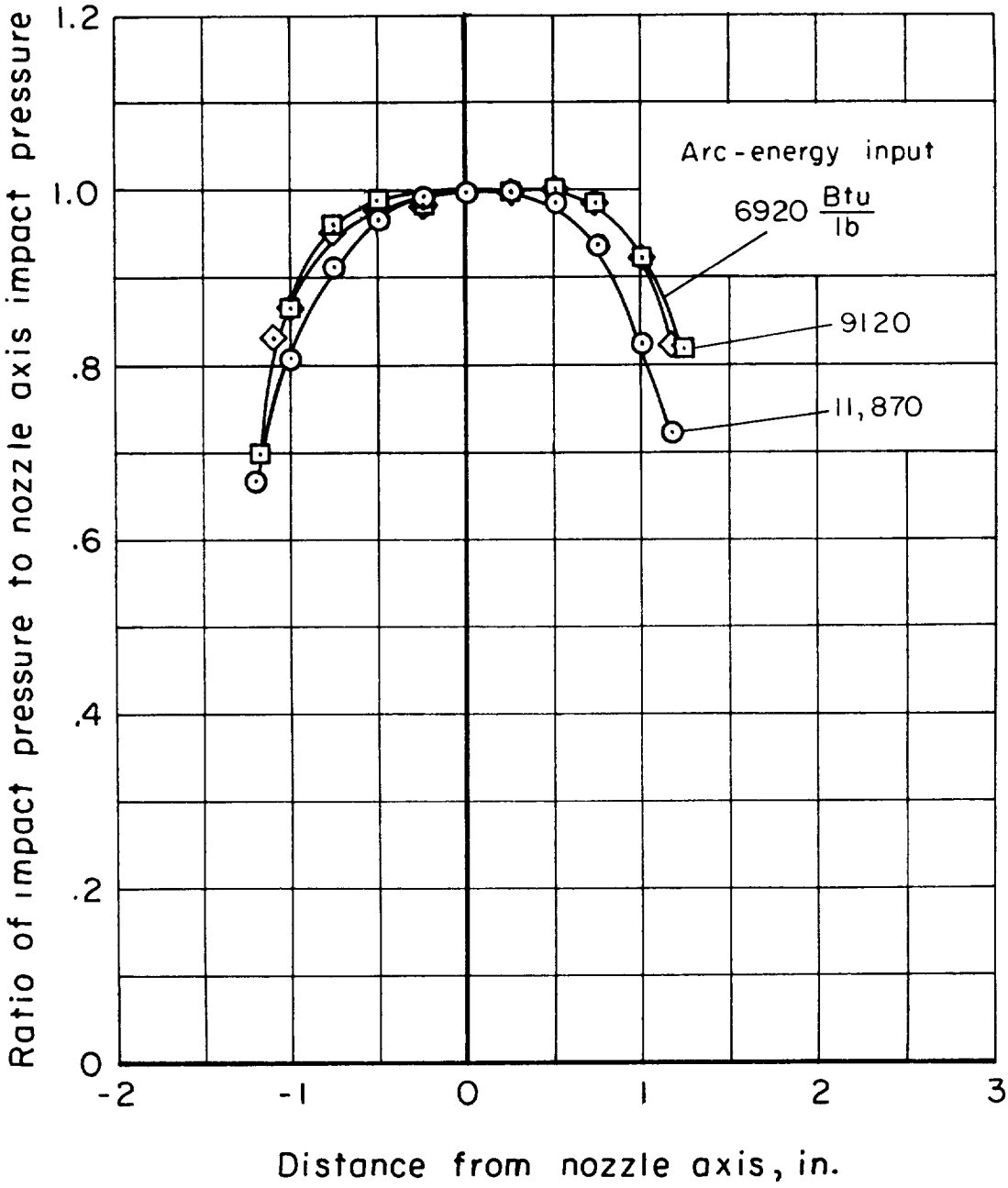

Figure 3.- Variation of ratio of impact pressure to nozzle axis impact pressure with distance from nozzle axis at various levels of arc-energy input.

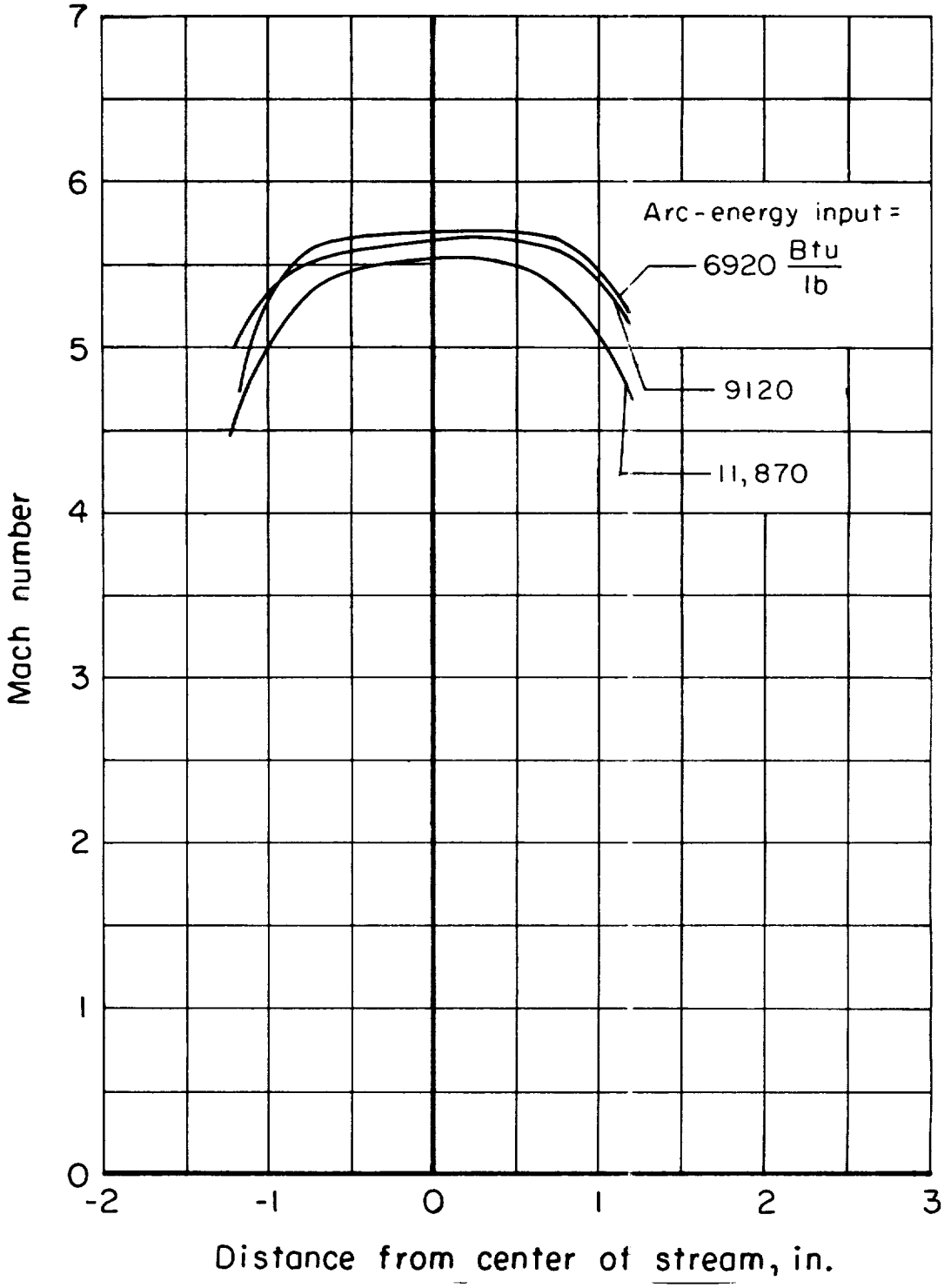

Figure 4.- Variation of Mach number with distance from nozzle axis at various levels of arc-energy input.

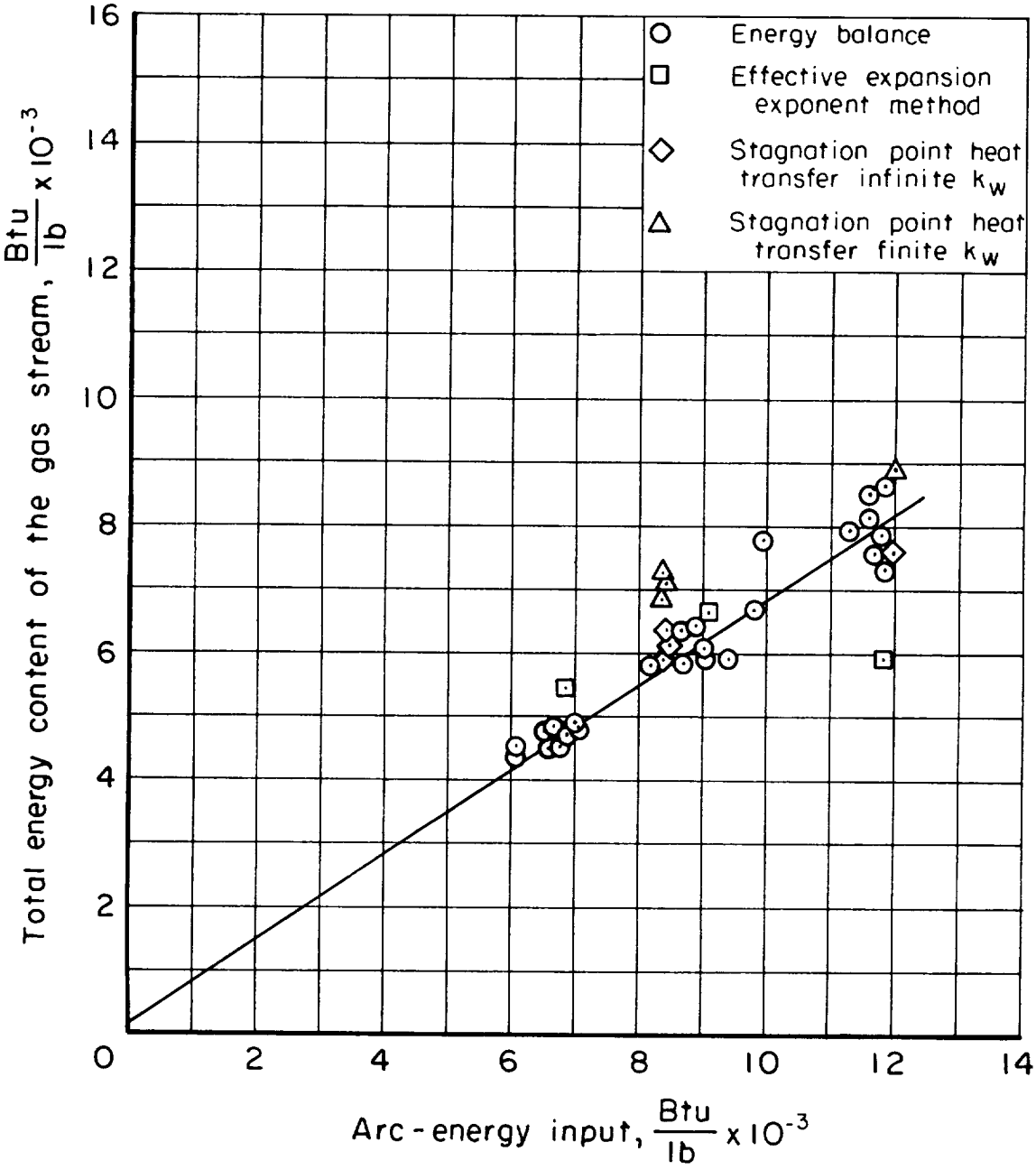

Figure 5. Variation of total energy content of the gas stream with arc-energy input.

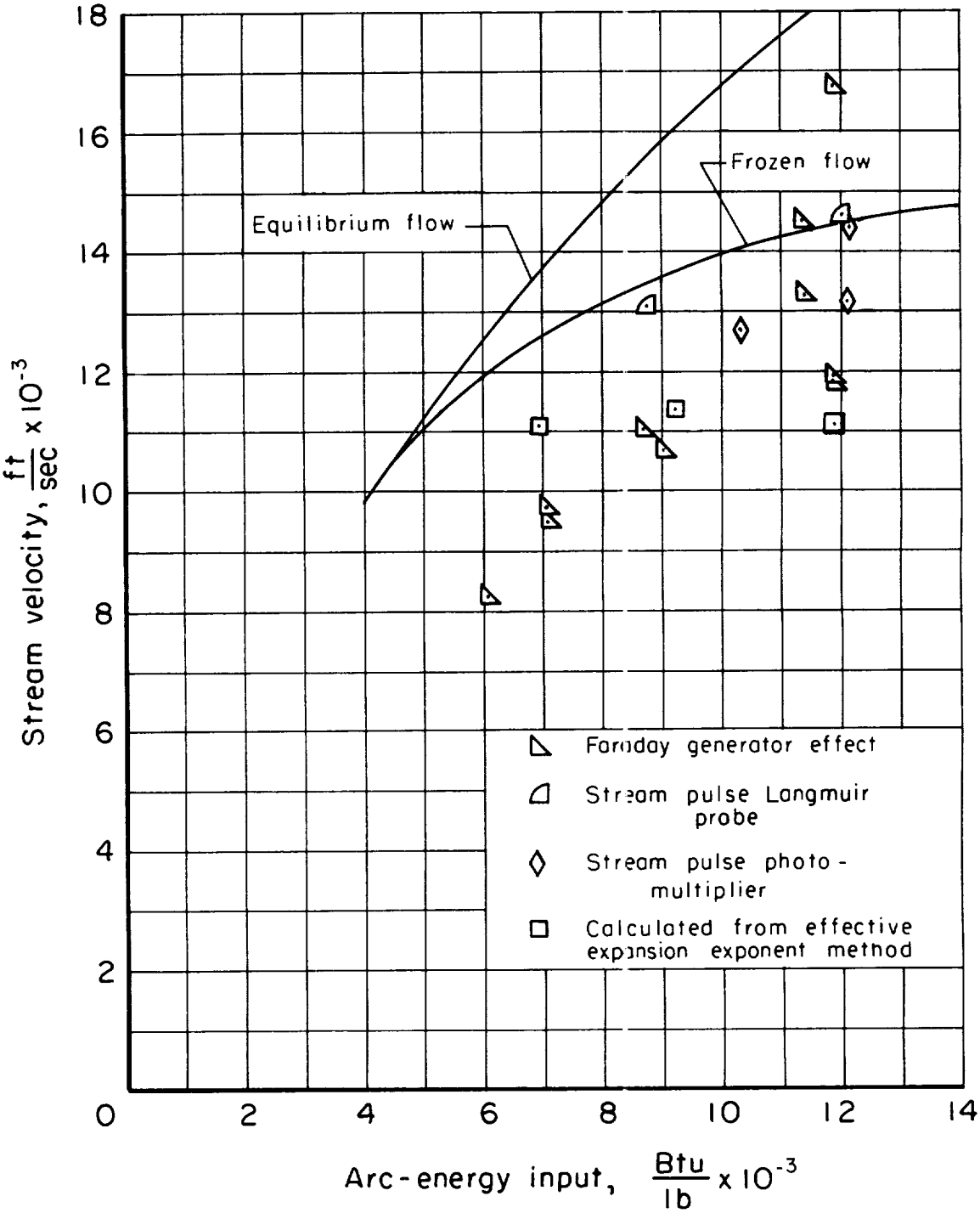

Figure 6.- Variation of stream velocity with arc-energy input.

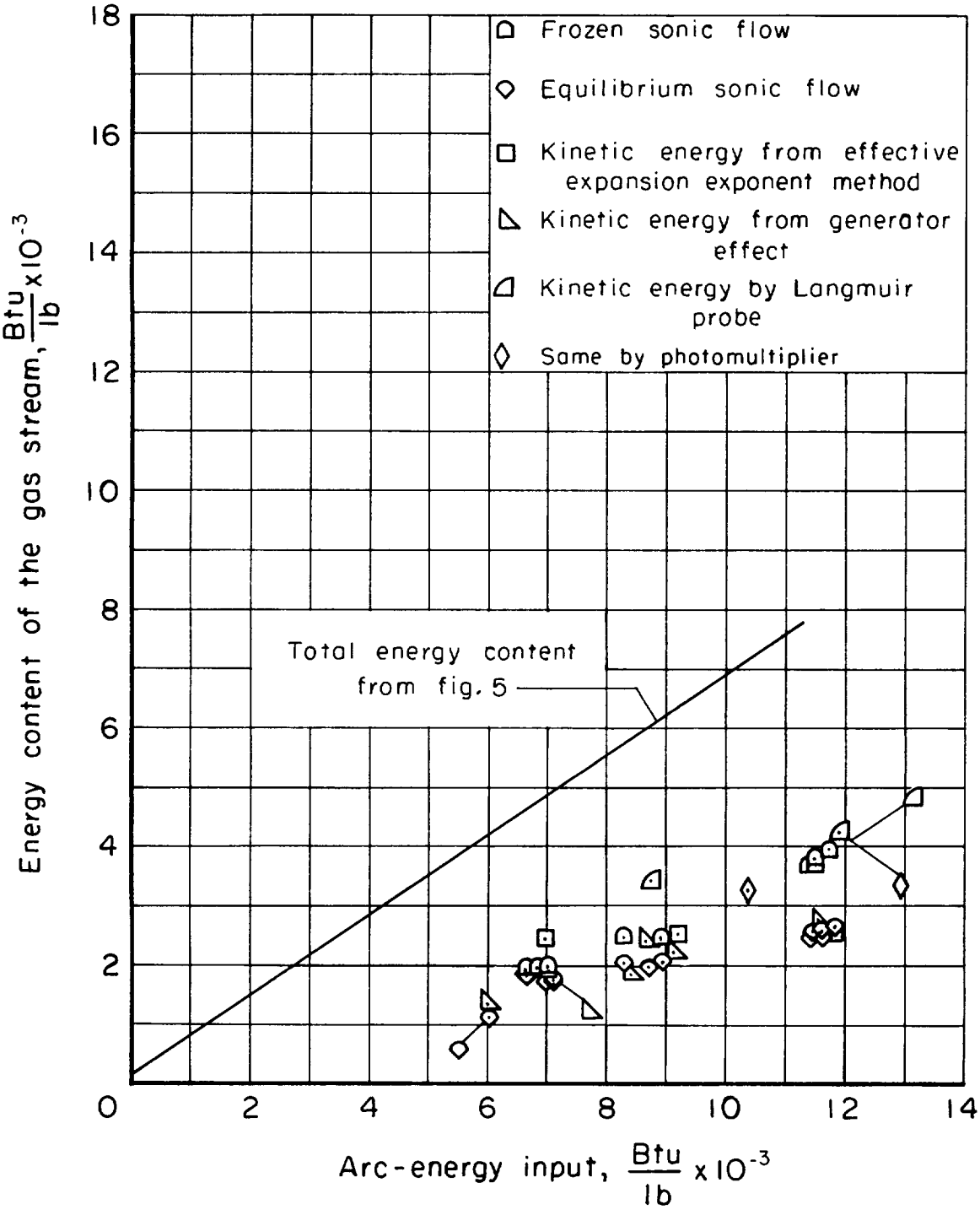

Figure 7.- Comparison of kinetic energy of the stream and the energy content deduced from sonic flow methods at various levels of arc-energy input.

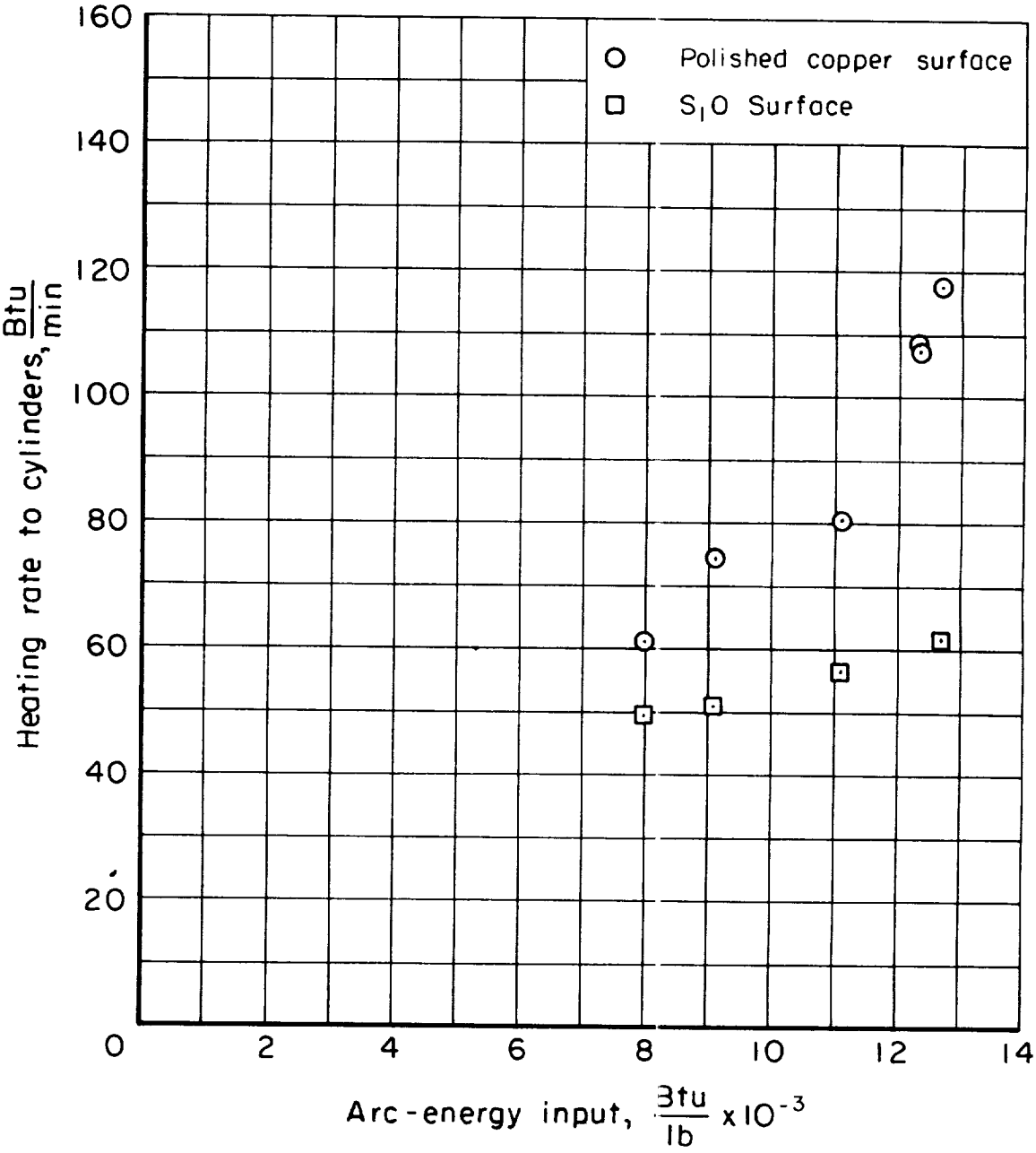

Figure 8.- Variation of heating rate to cylinders with arc-energy input.

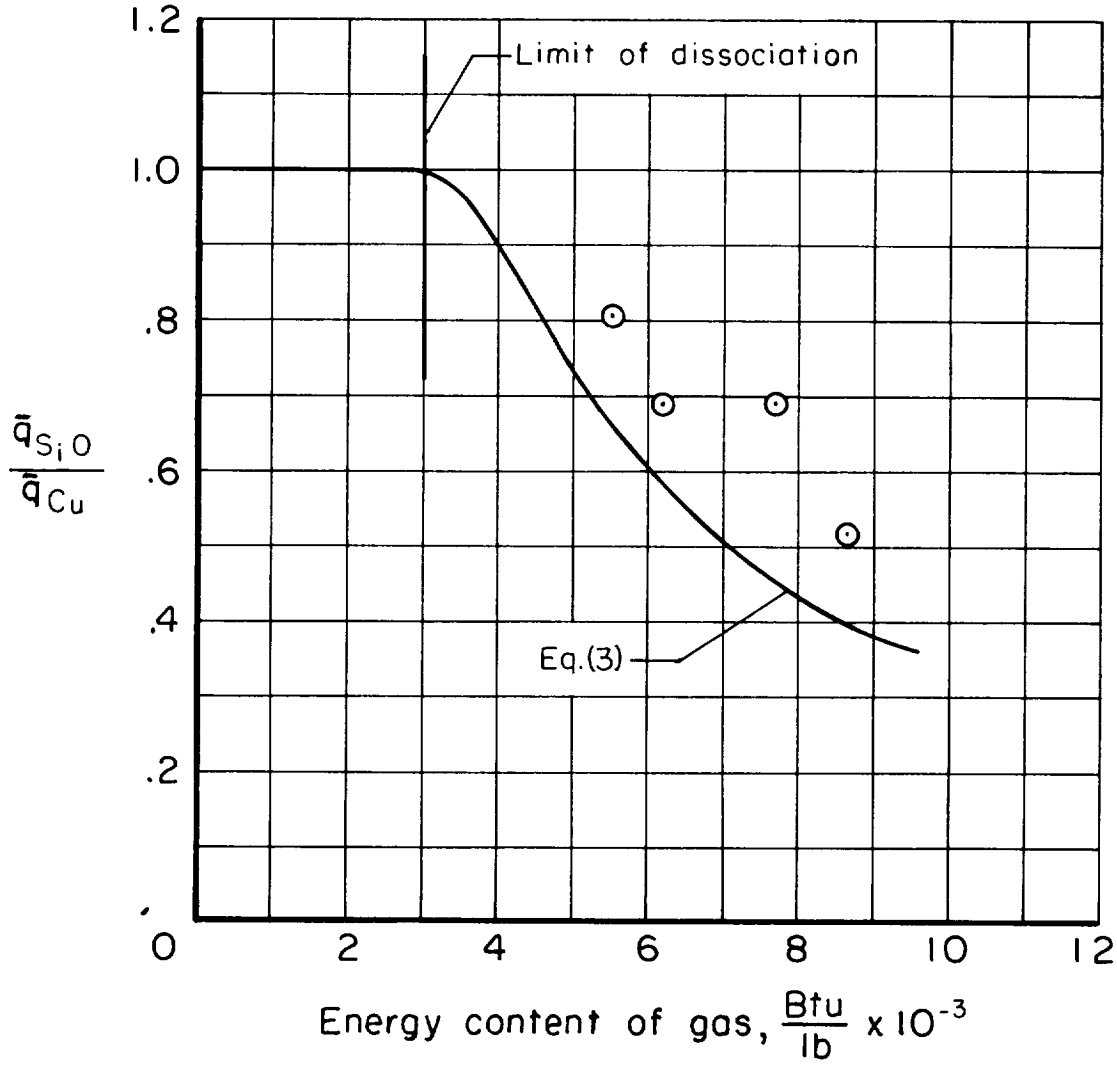

Figure 9.- Comparison of theoretical and experimental variation of catalytic effectiveness ratios of silicon monoxide and copper surfaces with stream enthalpy.